Andean Geology 50 (2): 167-180. May, 2023
doi: 10.5027/andgeoV50n2-3639

Andean Geology
www.andeangeology.cl

GEOLOGICAL NOTE

Integrated U-Pb and Hf zircon and whole-rock Nd isotopes studies of Devonian granitic rocks from Sierra de San Luis (Sierras Pampeanas, Argentina): Petrogenetic implications

***Juan A. Dahlquist[1], Matías M. Morales Cámera[1], Juan A. Moreno[2], Miguel A.S. Basei[3], Priscila Zandomeni[1], Gilmara Santos da Cruz[1]**

[1] *Centro de Investigaciones en Ciencias de la Tierra (CICTERRA), Consejo Nacional de Investigaciones Científicas y Técnicas, Facultad de Ciencias Exactas, Físicas y Naturales, Universidad Nacional de Córdoba, Av. Vélez Sársfield 1611, Ciudad Universitaria, X5016GCA Córdoba. Argentina.*
juan.andres.dahlquist@unc.edu.ar, matiasmmoralesc@unc.edu.ar, priscilazandomeni@gmail.com, gilmara.santos2010@gmail.com

[2] *Departamento de Mineralogía y Petrología, Universidad Complutense (UCM). José Antonio Novais 12, 28040 Madrid. Spain. juananmo@ucm.es*

[3] *Instituto de Geociências, Universidade de São Paulo. do lago 562 - Butantã, São Paulo - SP, 05508-080, Brasil. baseimas@usp.br*

** Corresponding author: juan.andres.dahlquist@unc.edu.ar*

ABSTRACT. Previous geochronological data indicate a protracted Devonian magmatic activity developed in the Sierra de San Luis, Sierras Pampeanas of Argentina, with three major crystallization events: 393±3, 384±2, and 377±2 Ma. Previously reported whole-rock Sm-Nd isotopes data define two average distinctive εNd_t values: -1.37 and -3.47, and they are consistent with new data presented here. The first signature is assumed for a parental magma with dominant metasomatized subcontinental lithospheric mantle (SCLM) source, whereas the second signature could represent a parental magma derived of a lower continental crust source hybridized with magmas of the first signature. Notably, the new zircon Hf isotopes performed on the same zircon domains that were previously dated, indicate that the contribution of the source was variable over time. *In situ* Hf in zircon is relevant to evaluate the compositional evolution of the Devonian granitic magmas in the Sierra de San Luis, since the high variability of the εHf_t values recorded in zircons indicate that the calculated εNd_t values for the samples can only be interpreted as a final picture of the petrogenetic process. Zircon Hf isotopes data suggest that the zircon crystallized from a magma with variable composition, recording two major events, yielding two εHf_t signatures: (1) -3.54 and (2) -6.85. A third composition, yield a less representative εHf_t value of -5.44, and represent a εHf_t signature (3).

Keywords: εHf_t and εNd_t values, U-Pb zircon geochronology, Petrogenetic process.

RESUMEN. Estudios integrados de isótopos de U-Pb y Hf en circón y Nd en roca total a partir de rocas graníticas devónicas en la Sierra de San Luis (Sierras Pampeanas, Argentina): implicancias petrogenéticas. Datos geocronológicos previos indican que una prolongada actividad magmática devónica se desarrolló en la Sierra de San Luis, Sierras Pampeanas de Argentina, con tres eventos de cristalización importantes: 393±3, 384±2 y 377±2 Ma. Datos previos de isótopos de Sm-Nd en roca total definen dos valores promedio distintivos de εNd_t: -1,37 y -3,47, los cuales son consistentes con los nuevos datos presentados aquí. La primera signatura es asumida para un magma parental

derivado de una dominante fuente de manto litosférico subcontinental metasomatizado (SCLM), mientras que la segunda signatura podría representar un magma parental derivado de una corteza continental inferior hibridado con un magma con la primera signatura. Notablemente, los nuevos datos de isótopos de Hf realizados en los mismos dominios de circón que se dataron previamente, indican que la contribución de la fuente fue variable a lo largo del tiempo. Los valores de Hf *in situ* en circón son relevantes para evaluar la evolución composicional de los magmas graníticos del Devónico en la Sierra de San Luis, ya que la alta variabilidad de los valores de εHf_t registrados en los circones, indica que los valores de εNd_t calculados para las muestras solo pueden ser interpretados como una imagen final del proceso petrogenético. Los datos de isótopos de Hf en circón sugieren que este mineral cristalizó a partir de un magma con composición variable, con dos eventos principales, que produjeron dos signaturas de εHf_t: (1) -3,54 y (2) -6,85. Una tercera composición arroja un valor de εHf_t menos representativo de -5,44, y equivale a una signatura de εHf_t (3).

Palabras clave: Valores de εHf_t y εNd_t, Geocronología U-Pb en circón, Procesos petrogenéticos.

1. Introduction

A feature of many studies is an implicit assumption that all zircons present in the host igneous rock are autocrysts, that is, crystallized from the surrounding melt. However, it has long been recognized that zircons present in an igneous rock can be inherited either from the surrounding country rock or source region (xenocrysts), or from earlier stages of magmatism in the magmatic source or in the plumbing system (antecrysts) (*e.g.*, Miller *et al.*, 2007).

Numerous works use different age populations of zircon to calculate an age, although individual ages show remarkable variations, displaying a relevant difference of *ca.* 15-20 Ma. This range of ages strongly suggest the presence of autocrysts and antecrysts in the crystallized rocks as indicated for different works (*e.g.*, Miller *et al.*, 2007; Siégel *et al.*, 2018; Dahlquist *et al.*, 2019; Moreno *et al.*, 2020). The presence of antecrysts suggests that the origin and emplacement processes of granitic magmas can last much longer than a million years. It has been recently shown by high precision geochronology that many plutons have been assembled in several magmatic pulses that can last several million years (*e.g.,* Tuolumne *suite* (USA), Coleman *et al.*, 2004; the Altiplano-Puna Volcanic Complex (Argentina-Bolivia-Chile), De Silva and Gosnold, 2007; Queensland (Australia), Siégel *et al.*, 2018; Cordillera Real (Bolivia), Iriarte *et al.*, 2021). In this context, more precise geochronological studies are needed to understand this problem and ultimately the development of the continental crust. On the other hand, during this extended petrogenetic process different chemical and/or isotopic changes are expected for the magmas, like those suggested by Kemp *et al.* (2007) for the granitoids of the Lachland Fold Belt, SW Australia, where the zircon of a same rock display a notable spectrum of εHf_t values (up to 10ε units).

LA-MC-ICP-MS zircon U-Pb ages from a sample (CHA-101) of the largest granitic unit from the Las Chacras-Potrerillos batholith, Sierra de San Luis, yield threes distinctive ages (outer error range): 393±3, 384±2, and 377±2 Ma, suggesting a protracted magmatic activity with three major crystallization events for this magmatism (Dahlquist *et al.*, 2019). Dahlquist *et al.* (2019) indicate that the older Late Devonian ages could indicate recycling of antecrystic zircons formed during early magma crystallization during the construction of a long-lived magma reservoir, while the youngest age is considered the emplacement age. This postulated protracted magmatic activity is appropriated to consider a prolonged zircon crystallization recording different magma compositions.

In this paper, we report the first study integrating previous *in situ* U-Pb and new Hf isotope data from magmatic zircon together with previous and new whole-rock Sm-Nd isotope data for two granitic rocks of the Las Chacras-Potrerillos and Renca batholiths, Sierra de San Luis, Argentina. This study is relevant to evaluate the compositional changes using Hf values of zircon crystallized in granitic magmas, derived from two potential sources previously identified using whole-rock Nd isotopes data.

2. Devonian granitic foreland magmatism in Sierra de San Luis

A Devonian foreland magmatism is located between 31° 00′ and 33°30′ S, in the present-day Sierras de Córdoba and Sierra de San Luis of Argentina. (Fig. 1). This Devonian foreland magmatism is characterized by development of large intracontinental batholiths and the absence of arc magmatism on the western margin of the plate at this latitude (Dahlquist *et al.*, 2021). Emplacement of these magmas took place mainly into metamorphic basement formed

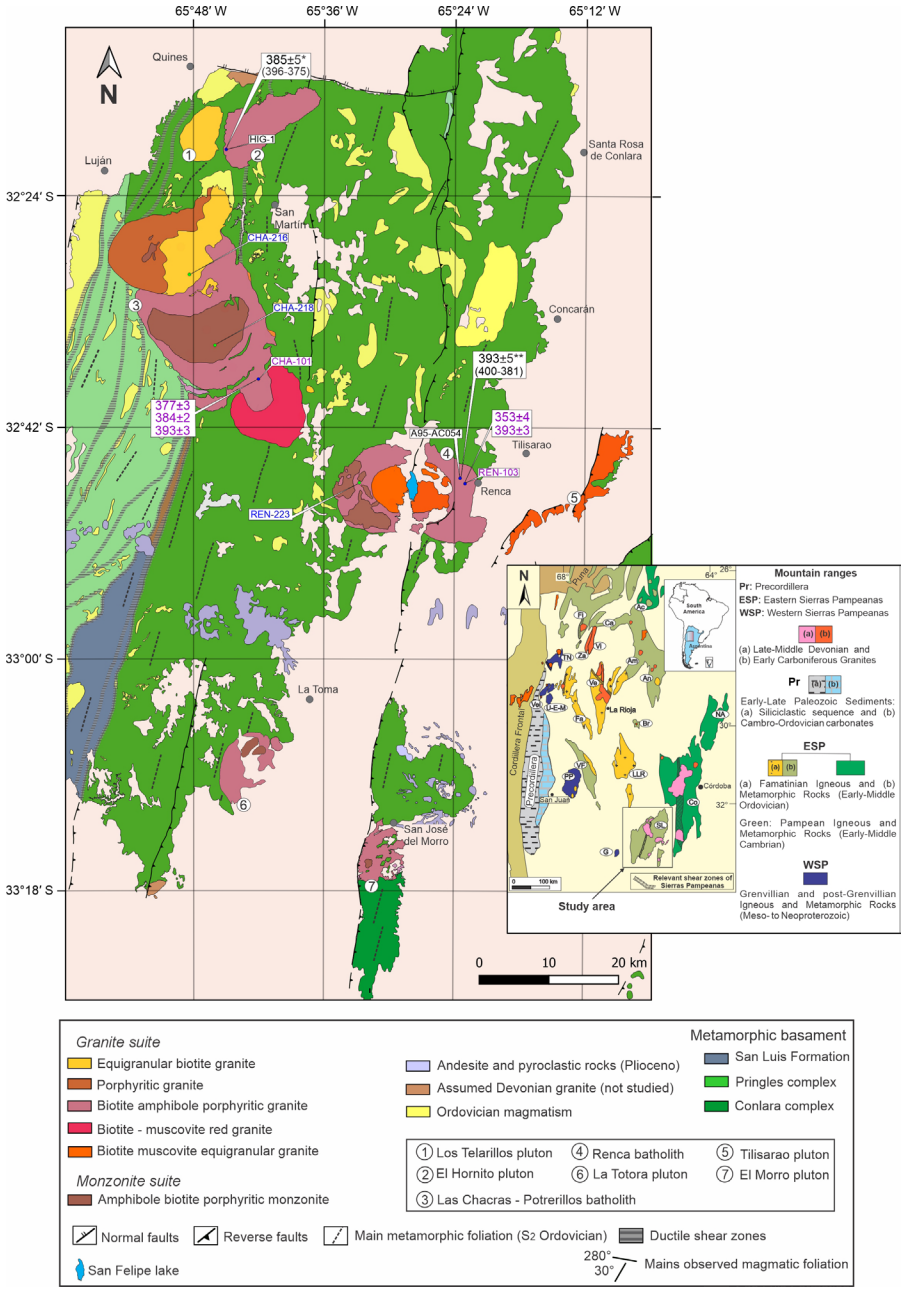

FIG. 1. Simplified regional geological map of Sierra de San Luis displaying the studied granitic pluton included in the Las Chacras-Potrerillos and Renca batholiths and eastern plutons (modified from López de Luchi *et al.*, 2017; Morosini *et al.*, 2017; Dahlquist *et al.*, 2019). The studied samples were georeferenced using GIS software. Geochronological data for the studied samples and those referred in the text are included. In violet letter, geochronological data for the studied samples in this work. Previous geochronological data: *Muñoz *et al.* (2022), **Stuart-Smith *et al.* (1999). In bracket, range of determined age values. *Granite* and *Monzonite suites* are from López de Luchi *et al.* (2017). In blue letter samples with whole-rock Sm-Nd data reported in this work. *Inset*: Simplified regional geological map of central NW Argentina, showing the Devonian and Carboniferous magmatic development of the pre-Andean margin of SW Gondwana (Dahlquist *et al.*, 2018a, 2021) and the location of the studied granitoids. The mountain ranges are: **Co:** Córdoba, **NA:** Norte-Ambargasta, **SL:** San Luis, **G:** El Gigante, **LLR:** llanos de la Rioja, **VF:** valle Fértil, **PP:** Pie de Palo, **Br:** Brava, **An:** Ancasti, **Ve:** Velasco, **Fa:** Famatina, **U-E-M:** Umango-Espinal and Maz, **Am:** Ambato, **Vi:** Vinquis, **TN:** Toro Negro, **Za:** Zapata, **Be:** Belén, **Ca:** Capillitas, **Fi:** Fiambalá, **Ac:** Aconquija. **Vel:** cerro Veladero, referred to in the text.

during the Early Paleozoic Pampean and Famatinian orogenies (*e.g.*, Steenken *et al.*, 2011; Casquet *et al.*, 2018; Muñoz *et al.*, 2022). Devonian granites were discordantly emplaced in medium to high grade metamorphic country rocks (*e.g.*, Rapela *et al.*, 1998; Christiansen *et al.*, 2019) overprinted by a strong shear deformation leading to formation of a major mylonitic belt (Siegesmund *et al.*, 2004; Semenov and Weinberg, 2017 and references therein).

Integrated petrological, geochemical, isotopic, and U-Pb zircon geochronology data of this Devonian foreland magmatism of Sierras Pampeanas of Argentina, represented for the granitoids of Sierras de Córdoba and San Luis (Fig. 1), have been discussed in previous works (*e.g.*, López de Luchi *et al.*, 2017; Muñoz *et al.*, 2022; Dahlquist *et al.*, 2019, 2021 and references therein). Recently, a geodynamic framework for the generation of the Devonian magmatism foreland was postulated by Dahlquist *et al.* (2021), and an overview of the origin of these magmas can be found in that work.

According to López de Luchi *et al.* (2017), the granitic rocks of the Sierra de San Luis define two distinctive *suites,* called *Monzonite suite* (<65 wt%) and *Granite suite* (>65 wt%), emplaced in shallow conditions, ranging from 3.3 to 4.7 kbar (Iannizzotto and López de Luchi, 2012; Muñoz *et al.*, 2022). As noted by López de Luchi *et al.* (2017), classification of the studied Devonian granitoids is subject to debate because they are I- to A-type hybrid granites. Whole-rock Nd isotopes data have been reported by some authors (*e.g.*, López de Luchi *et al.*, 2017; Dahlquist *et al.*, 2019), but zircon Hf isotopes data remain absent for these granitic rocks. Based on whole-rock geochemistry and Sm-Nd isotopes data, previous work identifies two sources for the parental magmas: **1**) metasomatized subcontinental lithospheric mantle (SCLM) and **2**) a lower continental crust source hybridized with magmas derived from SCLM (López de Luchi *et al.*, 2017; Dahlquist *et al.*, 2019).

The first U-Pb SHRIMP zircon age was reported by Stuart-Smith *et al.* (1999) for a granitoid of the Renca batholith. Subsequently, U-Pb SHRIMP and LA-MC-ICP-MS zircon ages were reported by Dahlquist *et al.* (2019) for granitic rocks of the Las Chacras-Potrerillos and Renca batholiths, respectively. Recently, a U-Pb LA-MC-ICP-MS zircon age for the El Hornito pluton was reported by Muñoz *et al.* (2022).

As noted in Section 1, a common feature of a studied granitic rock from the Las Chacras-Potrerillos batholith is that the individual U-Pb zircon ages mostly vary between *ca.* 393 and 377 Ma, displaying a relevant time spam of *ca.* 15 My (previous and new U-Pb zircon LA-MC-ICP-MS data are indicated in Fig. 1). The SHRIMP zircon age reported by Stuart-Smith *et al.* (1999) is a weighted mean age of 393±5 Ma, with individual values ranging from 405 to 381 Ma, whereas the LA-MC-ICP-MS zircon age of Muñoz *et al*. (2022) is a Concordia age of 385±2 Ma with a moderately high MSWD=2.2 (1σ**,** recalculated age to 2σ is 385±5, n=9, with MSWD=2.1, and it is shown in Fig. 1), with individual values varying between 396 and 375 Ma that evidence a relevant difference of *ca.* 20 My. Notably, the individual U-Pb zircon values reported by Stuart-Smith *et al.* (1999) are mostly close to 400 Ma, but similar individual values have not been found in our analyses and are also absent in the work of Muñoz *et al.* (2022).

3. Analytical methodology

New Nd isotopic analyses for the samples CHA-216, CHA-218, and REN-223 (location in Fig. 1), representative of the main granitic units of the Las Chacras-Potrerillos and Renca batholiths, were carried out at the Geochronology and Isotope Geochemistry Centre of the Complutense University of Madrid, Spain. Isotopic analyses were made on an automated multicollector TIMS-PhoenixR mass spectrometer. Analytical uncertainties are estimated to be 0.006% for $^{143}Nd/^{144}Nd$ and 0.1% $^{147}Sm/^{144}Nd$. Replicate analyses of the JNdi-1 Nd-isotope standard yielded an average $^{143}Nd/^{144}Nd$ ratio of 0.512108±0.000012 (2σ) with n=6. $^{143}Nd/^{144}Nd$ was normalized to $^{146}Nd/^{144}Nd$=0.7219. Sm, and Nd concentrations in ppm were determined by ICP-MS to calculate the $^{147}Sm/^{144}Nd$ ratios.

SiO_2, and Sm and Nd data for the samples CHA-218, CHA-216, and REN-223 are reported in table 1, were analyzed at the Geosciences Institute of the University of Campinas (UNICAMP), Brazil. The analyses were led on a Philips PW 2404 X-ray fluorescence spectrometer and on a Thermo (Xseries2) quadrupole ICP-MS equipped with Collision Cell Technology (CCT), respectively, using procedures described in Cardoso *et al.* (2019). Analytical information can be found in Cardoso *et al.* (2019). Previous and new Sm-Nd data are reported in table 1.

TABLE 1. PREVIOUS AND NEW WHOLE-ROCK Sm-Nd ISOTOPES DATA FOR THE GRANITIC PLUTON OF THE *GRANITE* AND *MONZONITE SUITE* OF SIERRA DE SAN LUIS.

Samples	SiO_2	Sm ppm	Nd ppm	$^{147}Sm/^{144}Nd$	$(^{143}Nd/^{144}Nd)_{today}$	$(^{143}Nd/^{144}Nd)_t$	εNdt	T_{DM}[1] (Ma)
Monzonite Suite (>65 wt%)								
AH26	57.55	22.6	142.0	0.0961	0.512312	0.512312	-1.48	1.25
173S	59.78	17.6	113.4	0.0937	0.512308	0.512074	-1.45	1.25
CHA-218[2]	64.72	12.1	74.8	0.0978	0.512338	0.512095	-1.18	1.22
Granite Suite (<65 wt%)								
REN-223[2]	66.23	9.3	54.9	0.1019	0.512231	0.511977	-3.47	1.41
CHA-101[3]	68.66	12.5	69.9	0.1083	0.512265	0.511995	-3.12	1.38
REN-103[3]	69.39	4.32	25.4	0.1026	0.512347	0.512092	-1.23	1.22
AH20	68.22	30.6	173.8	0.1064	0.512258	0.511994	-3.03	1.38
SLC1	68.80	12.5	76.1	0.0995	0.512240	0.511992	-3.18	1.38
SLC2	71.80	8.4	48.1	0.1055	0.512239	0.511976	-3.49	1.41
M60	67.66	6.7	42.9	0.0950	0.512226	0.511990	-3.23	1.39
PG1	70.80	9.3	58.4	0.0960	0.512316	0.512077	-1.52	1.25
CHA-216[2]	71.60	4.9	26.5	0.1118	0.512276	0.512001	-3.08	1.37
EG3	72.80	8.0	51.2	0.0949	0.512242	0.512006	-2.92	1.36
SLC7	76.00	6.1	23.1	0.1592	0.512373	0.511978	-3.47	1.41
SLC8	76.10	5.2	26.4	0.1181	0.512388	0.512094	-1.20	1.22
55	71.52	5.3	29.2	0.1091	0.512244	0.511972	-3.57	1.41
50	73.45	5.2	28.6	0.1103	0.512226	0.511951	-3.98	1.45
57	73.64	4.6	25.9	0.1085	0.512213	0.511943	-4.14	1.46
MR5	75.07	2.9	15.8	0.1109	0.512216	0.511940	-4.19	1.47
M01	72.16	15.6	82.8	0.1139	0.512252	0.511969	-3.64	1.42

The decay constant used in the calculations is $\lambda^{147}Sm=6.54\times10^{-12}$ year^{-1} recommended by the IUGS Subcommission for Geochronology (Steiger and Jäger, 1977). Epsilon Nd (εNd) values were calculated relative to a chondrite present day: $(^{143}Nd/^{144}Nd)_{today}$ CHUR=0.512638; $(^{143}Sm/^{144}Nd)_{today}$ CHUR=0.1967. *t*=time used for the calculation of the isotopic initial ratios. εNd_t values calculated for the crystallization age (t): 385 Ma. [1]T_{DM}= calculated according to De Paolo *et al.* (1991). The previous whole-rock Sm-Nd isotopes data from López de Luchi *et al.* (2017), excluding isotopes data of Sato *et al.* (2001) reported in that work because the location of the analyzed samples is unknown and the Devonian age is uncertain (see Morosini *et al.*, 2017, Fig. 2 in this work). [2]Values reported in this work. [3]Values reported by Dahlquist *et al.* (2019).

Zircon Hf-isotopes data were obtained from the samples CHA-101 and REN-103 (*Granite suite*) previously dated by Dahlquist *et al.* (2019). Description about the characteristics of the analyzed zircon grains as well as the separation and concentration mineral is carried out in Dahlquist *et al.* (2019). *In situ* LA-MC-ICP-MS Lu-Hf isotope analyses were also conducted at the Geochronological and Isotopic Geochemical Research Centre, Sao Paulo University, Brazil using a Laser Analyte Excite-Photon Machines (Teledyne) - 193 nm coupled to a Thermo-Finnigan Neptune MC-ICP-MS with nine Faraday collectors. The Lu-Hf isotopic analyses reported here were performed on the same zircon domains that were previously dated. Complete analytical description as well as typical laser operating conditions, analysis routine, correction data from Morales Cámera *et al.* (2020). Lu-Hf results are reported in table 2.

TABLE 2. Hf ISOTOPE DATA FOR IGNEOUS DATED ZIRCON FROM THE SAMPLES CHA-101 AND REN-203 (*GRANITE SUITE*).

Sample CHA-101							
Grain spot	**t**	**$^{176}Hf/^{177}Hf$**	**±2 σ**	**$^{176}Lu/^{177}Hf$**	**±2 σ**	**ƐHf (t)**	**T_{DM} (Ga)**
1.1	380	0.28219	0.00008	0.0015	0.0001	-12.61	2.11
3.1	394	0.28235	0.00002	0.00101	0.00002	-6.52	1.74
4.1	376	0.28244	0.00006	0.00097	0.00001	-3.71	1.55
6.1	393	0.28227	0.00009	0.00171	0.00007	-9.56	1.93
9.1	383	0.28239	0.00001	0.00077	0.00001	-5.28	1.65
9.2	384	0.28232	0.00006	0.00119	0.00002	-7.85	1.82
11.1	386	0.28241	0.00002	0.00086	0.00002	-4.53	1.61
13.1	393	0.28245	0.00002	0.000753	0.000006	-2.94	1.51
14.1	377	0.28245	0.00009	0.00105	0.00005	-3.36	1.53
15.1	383	0.28238	0.00001	0.000588	0.000002	-5.59	1.67
16.1	379	0.28242	0.00003	0.0006	0.00002	-4.27	1.59
19.1	377	0.2823	0.0002	0.0014	0.0001	-8.76	1.87
20.1	398	0.28243	0.00001	0.00061	0.00002	-3.50	1.55
21.1	391	0.28243	0.00001	0.00061	0.00002	-3.65	1.56
24.1	377	0.2825	0.0001	0.00096	0.00004	-1.57	1.41
30.1	386	0.2823	0.0001	0.00111	0.00007	-8.49	1.86
Sample REN-103							
Grain spot	**t**	**$^{176}Hf/^{177}Hf$**	**±2 σ**	**$^{176}Lu/^{177}Hf$**	**±2 σ**	**ƐHf (t)**	**T_{DM} (Ga)**
1.1	383	0.28247	0.00004	0.00081	0.00002	-2.46	1.48
2.1	343	0.28241	0.00003	0.00089	0.00003	-5.47	1.63
5.1	356	0.2824	0.00002	0.00118	0.00009	-5.61	1.65
6.1	393	0.2824	0.00001	0.00091	0.00003	-4.75	1.63
7.1	395	0.2821	0.0002	0.0014	0.0001	-15.45	2.30
10.1	355	0.28245	0.00003	0.000812	0.000004	-3.77	1.54

t=crystallization age of the CHA-101 and REN-103 samples reported by Dahlquist *et al.* (2019). T=model age. A two-stage continental model (T_{DM}) was calculated using the initial $^{176}Hf/^{177}Hf$ of zircon and the $^{176}Lu/^{177}Hf$=0.015 ratio for the lower continental crust (Griffin *et al.*, 2004). Decay constant for ^{176}Lu of $1.867x10^{-11}$ a^{-1} was used (Söderlund *et al.*, 2004). The present-day chondritic (CHUR) ratios of $^{176}Hf/^{177}Hf$=0.282772 and $^{176}Lu/^{177}Hf$=0.0332 from Blichert-Toft and Albarede (1997) were adopted to calculate εHf values.

4. Results

4.1. U-Pb LA-MC-ICP-MS zircon ages

As referred in Section 1, a common characteristic of the studied sample CHA-101 (as well as other samples referred in Section 2) is the relevant time spam of *ca.* 15 My display between the individual U-Pb zircon analyses. Therefore, we report combined diagrams as suggested by Siégel *et al.* (2018) to discriminate age populations, in order to identify zircon antecrysts and autocrysts (*e.g.*, combined linearized probability plot and weighted mean age diagrams). To distinguish autocrysts from antecrysts

(or xenocrysts), we use a two-stage approach. First, the number of zircon age populations are defined using linearized probability plots to identify younger and older age analyses. Any data points that are not within the calculated regression line are excluded from the populations. Linearized probability plots therefore provide a visual basis whereby multiple zircon age populations can be recognized. Is relevant to clarify that for discriminating age populations it is mandatory to work with a large group of data, thus the obtained results will have statistical significance. Subsequently, weighted mean ages of each zircon age population can then be calculated and interpreted as autocrysts, antecrysts or xenocrysts.

Three age groups from sample CHA-101 were used by Dahlquist *et al.* (2019) to calculate three consistent weighted mean ages (outside error limits): 379±2, 385±2, and 392±2 Ma (Fig. 2A-C). Notably, when a weighted mean is calculated using all the individual U-Pb zircon data from sample CHA-101, an unacceptable MSDW=13 is obtained (Fig. 2D). Using previous geochronological data from Dahlquist *et al.* (2019) we report new linearized probability plot (Isoplot/Ex 4.15 Ludwig, 2008) diagrams (Fig. 3A-D), where three age groups as those reported by Dahlquist *et al.* (2019) are clearly distinguished using now mathematical support. In addition, a linearized probability plot diagram considering the whole data-set from sample CHA-101 yields a regression line with a relatively high error (±14 Ma) for the calculated slope (Fig. 3D). The figure 3A-D reported in this work gives robustness to previously calculated ages, and confirm a protracted Devonian magmatic event in Sierra de San Luis.

4.2. Sm-Nd whole-rock isotope data

Previous whole-rock Sm-Nd isotope data reported by López de Luchi *et al.* (2017) indicate that the magmatic *suites* in Sierra de San Luis have two distinctive average εNd_t (t=inferred mean crystallization age, 385 Ma). The εNd_t

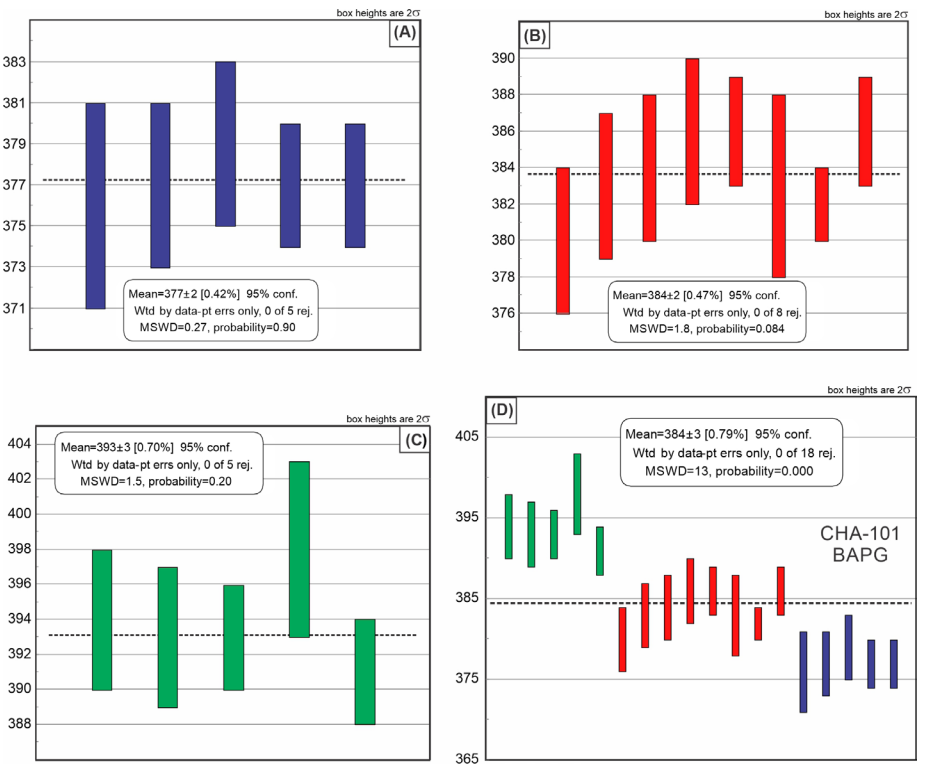

FIG. 2. **A-D.** *Weighted mean ages* diagrams, after Dahlquist *et al.* (2019). Considering the whole dataset, sample CHA-101 (Biotite amphibole porhyritic unit, BAPG) yields an age with a high MSWD value of 13. Conversely, the three populations previously distinguished yield ages with appropriate MSWD values. *Inset* shows the calculated mean age.

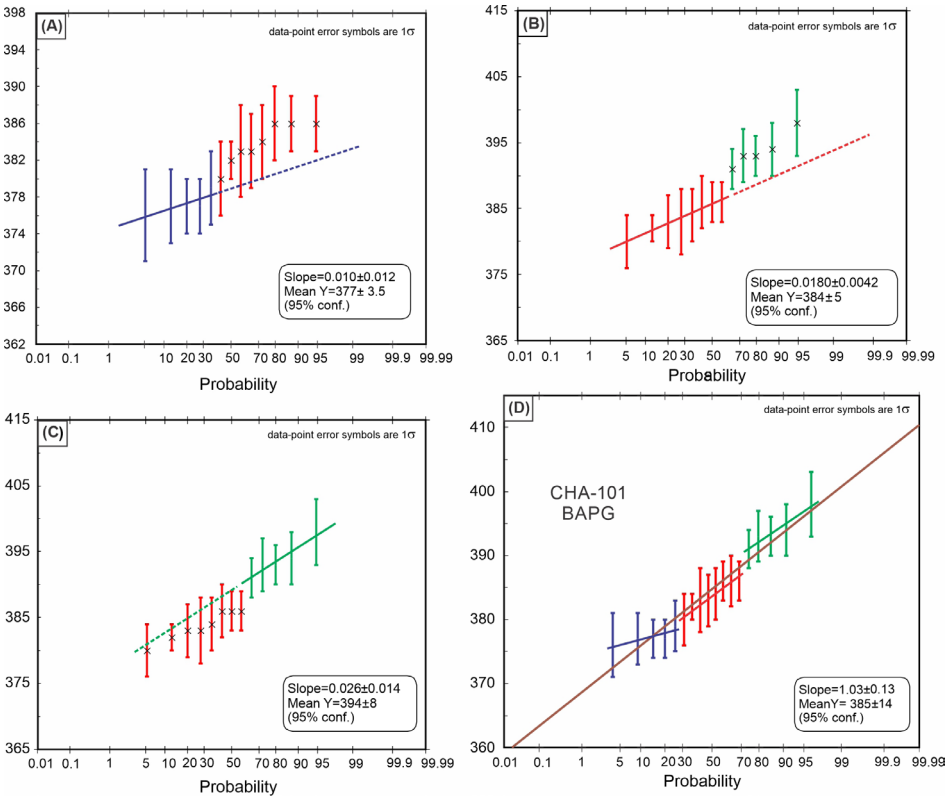

FIG. 3. **A-D.** *Linearized probability plots* diagrams for the sample CHA-101 (BAPG unit, Las Chacras-Potrerillos batholith) using individual zircon U-Pb ages. Taking as a whole (**D**) sample CHA-101 yields a regression line with a relatively high error (±14 Ma) for the calculated slope. By contrast, using the three age populations a lower error is obtained for the calculated slopes. *Inset* shows the slope line regression and calculated age, "X" represents excluded data.

values for the *Monzonite suite* ranges from -1.18 to -1.48 (n=3), with an average of -1.37 (Table 1), whereas the εNd_t values for the *Granite suite* are variable, ranging from -1.20 to -4.19. However, the more negative εNd_t values are largely dominant in the *Granite suite*, with εNd_t values, ranging from -2.94 to -4.19 (n=14, average=-3.47) and from -1.20 to -1.50 (n=3, average -1.32), respectively (Table 1). Our new Sm-Nd data are consistent with the previous data as shown in table 1.

4.3. Hf in zircon isotope data

Using previous U-Pb zircon crystallization ages referred to above, εHf_t values were calculated from the new Lu-Hf zircon isotope data reported in table 2. Zircons from CHA-101 and REN-103 have variable but negative εHf_t values, ranging from -12.61 to -1.57 and from -4.75 to -2.46, respectively (Table 2). In the case of sample CHA-101, although all εHf_t values are negative, distinctive εHf_t values are obtained from the different individual ages (Fig. 4): εHf_t values mostly range from -1.57 to -4.27 (n=4, a single εHf_t value yield -8.76) for ages ranging from 376 to 379 Ma, and from -4.53 to -8.49 (n=5, a single εHf_t value yield -12.61) for ages ranging from 380 to 386 Ma. Older ages ranging from 391 to 393 Ma yield contrasting εHf_t values: -9.56, -3.65, and -2.94 (Table 2).

Two ages of 393±3 and 353±4 Ma were determined for the sample REN-103. The first age was interpreted as a crystallization age, whereas the younger age as the one resulted from a reheating event at *ca.* 350 Ma (see Dahlquist *et al.*, 2019 and Section 5.1). The εHf_t values from the younger individual ages (*i.e.*, ~350 Ma) vary between -3.77 and -5.61, and they are comparable to the εHf_t values reported for the Devonian crystallization ages of the samples CHA-101 and REN-103 (Table 2 and Fig. 5).

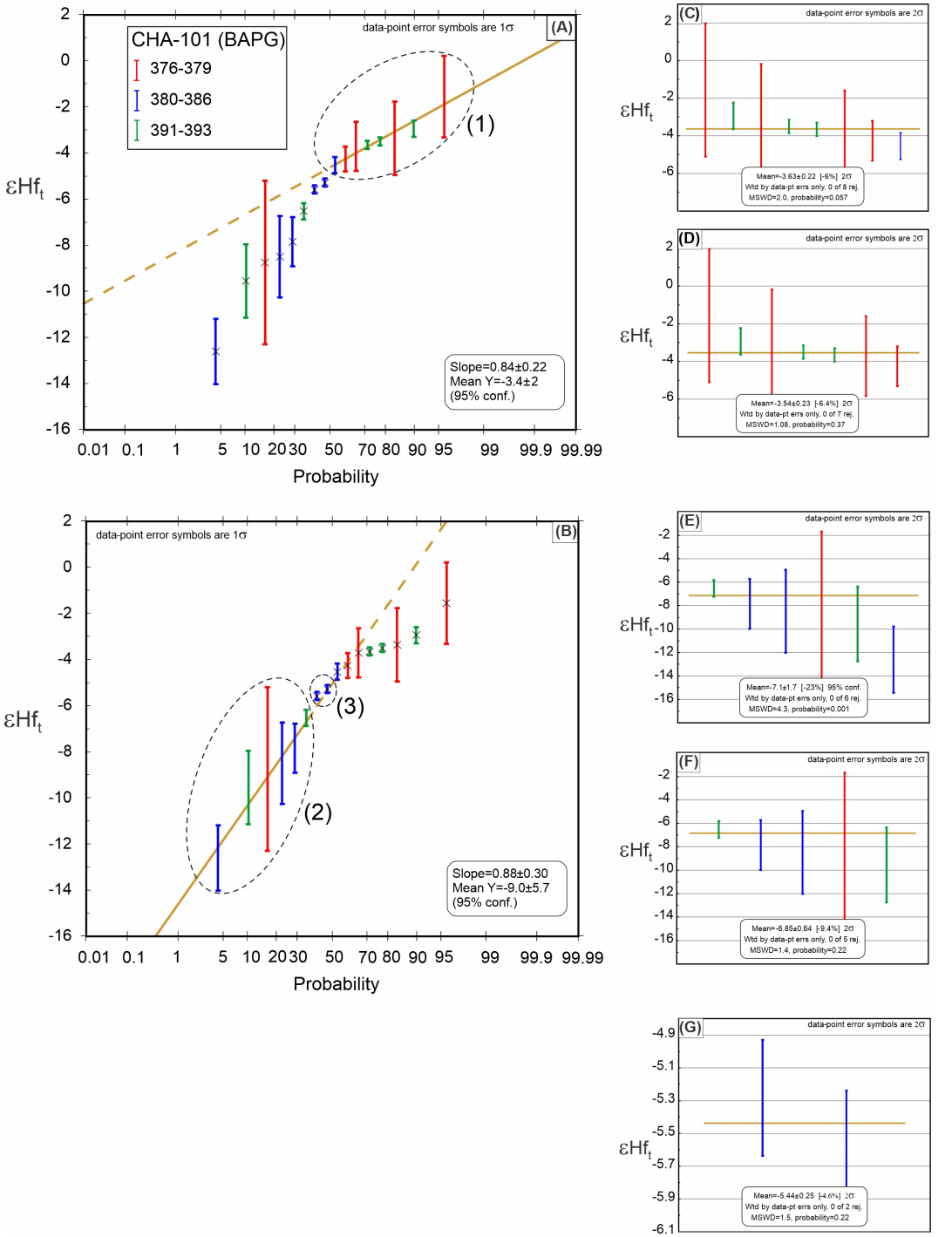

FIG. 4. **A-G.** *Linearized probability plots* and w*eighted mean* diagrams for sample CHA-101 using εHf$_t$ values. (**A**) and (**B**): two main εHf$_t$ populations define two εHf$_t$ signatures: (1) and (2), with mean values of -3.4 (n=7) and -9.0 (n=5), respectively. Two εHf$_t$ values of -5.28 and -5.59 define a less representative third population, which is referred as signature (3). (**C**) and (**D**), and (**E**) and (**F**), weighted mean for the recognized εHf$_t$ population in (**A**) and (**B**), respectively, yielding εHf$_t$ values of -3.54 and -6.85. (**D**) and (**F**) are preferred considering its MSWD. (**G**) weighted mean value for the third εHf$_t$ population, which yield a εHf$_t$ value of -5.44.

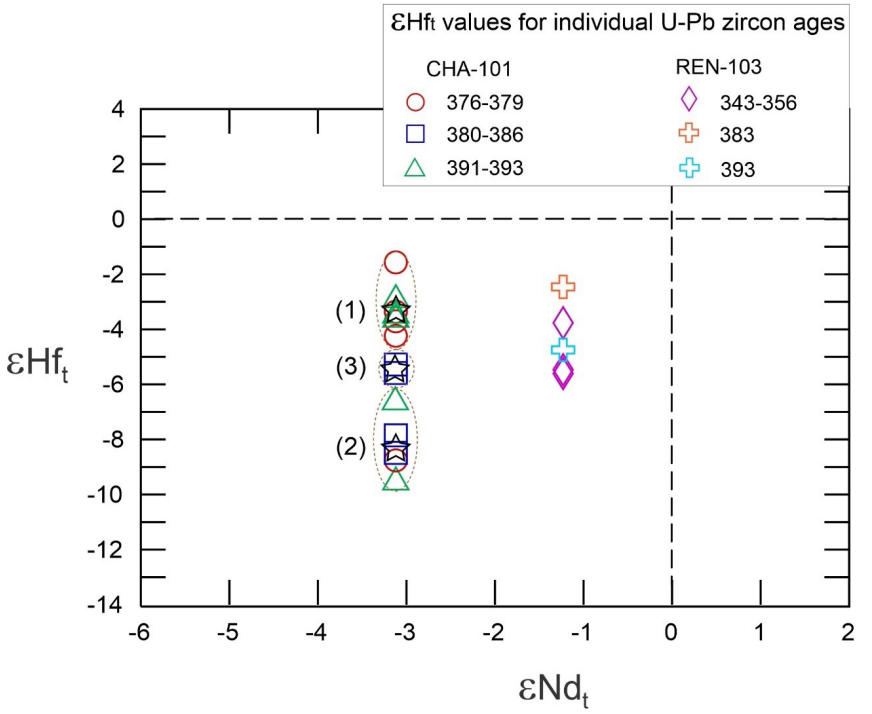

FIG. 5. εNd_t Age vs. εHf_t values for Devonian zircon from samples CHA-101 and REN-103 (BAPG units in the Las Chacras-Potrerillos and Renca batholiths), showing the initial epsilon Hf values as a function of the crystallization age. (1), (2), and (3) represent different εHf_t signatures previously recognized in figure 4 for sample CHA-101, with starts representing averages. In the average calculation for the εHf_t signature (2), the εHf_t value of -12.61 (Table 2) was exclude because this value was not considered in the weighted mean diagram of figure 4F (see discussion in the text). An "anomalous" εHf_t value of -15.45 (Table 2) for the sample REN-103 is not projected.

5. Discussion

5.1. U-Pb LA-MC-ICP-MS and SHRIMP zircon ages

Previous analyses (Section 4.1.) based on geochronological data, suggest a protracted magmatic activity during the building of the Las Chacras-Potrerillos batholith, and ongoing studies are focused on determining if this process is applicable to the Devonian magmatism of the Sierra de San Luis. This interpretation assumes a prolonged time in a deep hot zone maturation with a subsequent migration and emplacement of the granitic magma in shallow levels, as postulated by different authors (*e.g.*, Kemp *et al.*, 2007; Alasino *et al.*, 2017; Macchioli Grande *et al.*, 2020). This conceptual model is consistent with the studies of Dahlquist *et al.* (2018b) on the Veladero granitic stock in Western Sierras Pampeanas of Argentina (Fig. 1), which indicate that the granitic magma passed through ~10 km of continental crust (from *ca.* 17 to 7 km) before reaching its final emplacement level at shallow conditions.

On the other hand, as noted by Dahlquist *et al.* (2019) the younger age of 353±4 in the sample REN-103 (Renca batholith) is comparable to previous ages determined in micas crystallized in intragranitic pegmatites as well as cooling ages from biotite hosted in granitoids of the Las Chacras-Potrerillos batholith, being interpreted by Dahlquist *et al.* (2019) as the result of a subsequent heating event rather than a crystallization age. In particular, previous K-Ar ages from biotite crystallized in the Devonian granitoids of Sierra de San Luis, reveal cooling ages ranging from *ca.* 375 to 345 Ma (López de Luchi *et al.*, 2017). Therefore, younger ages than *ca.* 375 Ma are assumed as ages affected by Pb loss, with subsequent resetting of the isotopic clock.

5.2. *In situ* Hf zircon and whole-rock Nd isotopes

Based on whole-rock geochemistry and Sm-Nd isotopes data, previous works identify two sources for the parental magmas: **1**) metasomatized subcontinental lithospheric mantle (SCLM) and **2**) a lower continental crust source hybridized with magmas derived of SCLM (López de Luchi *et al.*, 2017; Dahlquist *et al.*, 2019). As described in Section 4.2, the average εNd_t value for the *Monzonite suite* is -1.37, and two distinctive εNd_t values are recognized for the samples of the *Granite suite*: -3.47 and -1.32. The second value is only observed in three samples (n=17) being undistinguishable of the εNd_t values reported for the *Monzonite suite*, and could indicates greater participation of the SCLM source in the hybridization process for these samples of the *Granite suite*.

The protracted magmatic activity postulated by Dahlquist *et al.* (2019) and verified in this work, along with the contribution of two sources for the parental magma of the *Granite suite*, is appropriated to postulate a prolonged zircon crystallization recording different magma compositions.

The identification of zircon Hf isotope populations can be performed qualitatively or using some mathematical method. In this case, the number of zircon Hf isotopic populations were defined using combined linearized probability plots and weighted mean calculations for sample CHA-101. The figures 4A-B, and 5 suggest that the zircon crystallized from a magma with variable composition, recording two major events, where the dominant εHf_t values are: (1) -3.54 (n=7) and (2) -6.85 (n=5, Fig. 4D-F). A third composition (3) yields a less representative εHf_t value of -5.44 (n=2, Fig. 4G). As shown in figure 4A and B, the signature (1) is dominant in older (391-393 Ma) and younger ages (376-379 Ma), whereas more negative εHf_t values (*i.e.*, signature 2 and 3) are mostly observed in intermediate ages (380-386 Ma).

Furthermore, the figure 4A-B show that during the prolonged petrogenetic process the magma underwent Hf isotopic compositional changes, with variable εHf_t values for the analyzed zircon of the sample CHA-101, which displays a single εNd_t value of -3.12 as shown in figure 5. Therefore, the εNd_t value for this sample CHA-101 can only be interpreted as a final picture of the petrogenetic process, and the compositional changes (and participation of different sources) cannot be assessed. Similar conclusions were obtained by Kemp *et al.* (2007) for the granitoids of the Lachlan Fold Belt of SW Australia, where the zircon of the studied samples derived from two postulated sources (SCLM and continental crust) yield different zircon Hf and O values for a given εNd_t value.

The zircon Hf values determined from sample REN-103 (Renca batholith) are insufficient to carry out a mathematical analysis like the one carried out for sample CHA-101 (Las Chacras-Potrerillos batholith). However, the epsilon Hf_t for zircons of sample REN-103 can be compared with those εHf_t values reported above for the sample CHA-101. The epsilon Hf_t of the sample REN-103 shows values comparable with the εHf_t of the sample CHA-101 (signature 1 and 3), but the εNd_t is -1.12 (Fig. 5). The limited analysis number from zircon of the sample REN-103 does not allow deeper interpretations, although preliminarily a dominant signature represented for (1) and (3) could be considered as well as the presence of a relatively homogeneous source, but excluding the signature (2), which indicate a marked contribution of continental crust.

The zircon εHf_t values for the younger ages from sample REN-103 ranging from 343 to 356 Ma, are comparable to those values reported for magmatic zircon (Fig. 5). This indicates that the U-Pb system would have been affected by the heating event but the $^{177}Hf/^{176}Hf$ ratio remained mostly unchanged, in a similar way as suggested by different works (*e.g.*, Farina *et al.*, 2014; Dahlquist *et al.*, 2020 and references therein). As it is known Hf and Pb are strongly compatible and incompatible in zircon, respectively. Consequently, it is expected that Hf will be preserved and Pb excluded from zircon grains, leading to Pb loss without eventual modification of the $^{177}Hf/^{176}Hf$ ratio.

6. Conclusions

1. The geochronological data strongly suggest the presence of zircon antecrysts and autocrysts with distinctive Hf composition. Combined individual U-Pb zircon ages and Hf analysis are relevant to evaluate the compositional evolution of granitic magmas in Sierra de San Luis.
2. Whole-rock Nd isotope data permit distinguishing two εNd_t signatures for the granitic rocks of the Las Chacras-Potrerillos and Renca batholiths: *ca.* -1.37 and -3.47. However, Hf zircon data from

sample CHA-101 indicate that the composition of the magma was not uniform and underwent variable isotopic changes during the petrogenetic process. In addition, it also seems to suggest the variable participation of different sources. In particular, the calculated εNd_t values for the samples CHA-101 and REN-103 can only be interpreted as a final picture of the petrogenetic process.

3. In general, two main εHf_t signatures were recognized from sample CHA-101: (1) -3.54 and (2) -6.85. A less representative εHf_t signature (3) of -5.44 is also recognized. The εHf_t signature (1) is mostly dominant in older and younger ages (376-379 and 391-393 Ma), whereas signature (2) and (3) are dominant for intermediate ages (380-386 Ma). Sample REN-103 shows similar values of εHf_t to those of the sample CHA-101 with signature (1) and (3) and suggest less compositional variation than sample CHA-101 during the petrogenetic process. A relatively homogeneous source, but excluding signature (2), could be inferred for the sample REN-103.
4. The age of 353 Ma calculated from some zircons of sample REN-103, indicates that the U-Pb system would have been affected by a heating event, but the $^{177}Hf/^{176}Hf$ ratio remained mostly unchanged.

Acknowledgments

The authors acknowledge financial support from PIP-0564 CONICET and PICT 2020 0378, Consolidar 2018 SECyT-UNC, and FAPESP 2018/06837-3 linked to Thematic Project FAPESP 2015/03737-0. We are very grateful to the external reviewer R. Iriarte for his appropriate revision. The Editor-in-Chief L.E. Lara is also acknowledged for his editorial handling. We appreciate the editing work of G. Blanco.

References

Alasino, P.H.; Larrovere, M.A.; Rocher, S.; Dahlquist, J.A.; Basei, M.A.S.; Memeti, V.; Paterson, S.R.; Galindo, C.; Macchioli Grande, M.; da Costa Campos Neto, M. 2017. Incremental growth of an upper crustal, A-type pluton, Argentina: evidence of a reused magma pathway. Lithos 284-285: 347-366.

Blichert-Toft, J.; Albarede, F. 1997. The Lu-Hf isotope geochemistry of chondrites and the evolution of the mantle-crust system. Earth Planetary Science Letters 148: 243-258.

Cardoso, C.D.; Ávila, C.A.; Neumann, R.; Oliveira, E.P.; Valeriano, C.M.; Dussin, I.A. 2019 A Rhyacian continental arc during the evolution of the Mineiro belt, Brazil: Constraints from the Rio Grande and Brumado metadiorites. Lithos 326-327: 246-264.

Casquet, C.; Dahlquist, J.A.; Verdecchia, S.O.; Baldo, E.G.; Galindo, C.; Rapela, C.W.; Pankhurst, R.J; Morales, M.M.; Murra, J.A.; Fanning, C.M. 2018. Review of the Cambrian Pampean orogeny of Argentina, a displaced orogeny formerly attached to the Saldania Belt of South Africa? Earth-Science Reviews 177: 209-225.

Christiansen, R.; Morosini, A.; Enríquez, E.; Muñoz, B.; Lince Klinger, F.; Martínez, M.P.; Ortiz Suárez, A.; Kostadinoff, J. 2019. 3D litho-constrained inversion model of southern Sierra Grande de San Luis: new insights into the Famatinian tectonic setting. Tectonophysics 756: 1-24.

Coleman, D.S.; Gray, W.; Glazner, A.F. 2004. Rethinking the emplacement and evolution of zoned plutons: geochronologic evidence for incremental assembly of the Tuolumne Intrusive Suite, California. Geology 32: 433-436.

Dahlquist, J.A.; Alasino, P.H.; Basei, M.A.S.; Morales Camera, M.; Macchioli Grande, M.; da Costa Campos Neto, M.C. 2018a. Petrological, geochemical, isotopic, and geochronological constraints for the Late Devonian-early Carboniferous magmatism in SW Gondwana (27°-32° LS): an example of geodynamic switching. International Journal of Earth Sciences 107: 2575-2603.

Dahlquist, J.A.; Alasino, P.H.; Basei, M.A.S.; Morales Camera, M.M.; Macchioli Grande, M.S.; da Costa Campos Neto, M.; García Larrecharte, M. 2018b. Recurrent intrusive episodes in the Paleozoic metasedimentary upper crust during the Early Carboniferous time: the Veladero granitoid stock and the peraluminous andesite. Journal of South American Earth Sciences 88: 80-93.

Dahlquist, J.A.; Macchioli-Grande, M.; Alasino, P.H.; Basei, M.A.S.; Galindo, C.; Moreno, J.A.; Morales Camera, M. 2019. New geochronological and isotope data for the Las Chacras-Potrerillos and Renca batholiths: a contribution to the middle-upper Devonian magmatism in the pre-Andean foreland (Sierras Pampeanas, Argentina). SW Gondwana. Journal of South American Earth Sciences 93: 348-363.

Dahlquist, J.A.; Galindo, C.; Morales Camera, M.M.; Moreno, J.A.; Alasino, P.H.; Basei, M.A.S.; Macchioli Grande, M. 2020. A combined zircon Hf isotope and whole-rock Nd and Sr isotopes study of Carboniferous

A-type granites, Sierras Pampeanas of Argentina. Journal of South American Earth Sciences 100: 102545.

Dahlquist, J.A.; Morales-Cámera, M.M.; Alasino, P.H.; Pankhurst, R.J.; Basei, M.A.S.; Rapela, C.W.; Galindo, C.; Moreno, J.A.; Baldo, E.G. 2021. A review of Devonian-Carboniferous magmatism in the central region of Argentina, pre-Andean margin of SW Gondwana. Earth-Science Reviews 221. doi: https://doi.org/10.1016/j.jsames.2020.102545

De Silva, S.L.; Gosnold, W.D. 2007. Episodic construction of batholiths: Insights from the spatiotemporal development of an ignimbrite flare-up. Journal of Volcanology and Geothermal Research 167: 320-335.

De Paolo, D.J.; Linn, A.M.; Schubert, G. 1991. The continental crustal age distribution; methods of determining mantle separation ages from Sm-Nd isotopic data and application to the Southwestern United States. Journal of Geophysical Research 96: 2071-2088.

Farina, F.; Stevens, G.; Gerdes, A.; Frei, D. 2014. Small-scale Hf isotopic variability in the Peninsula pluton (South Africa): the processes that control inheritance of source $^{176}Hf/^{177}Hf$ diversity in S-type granites. Contribution to Mineralogy and Petrology 168: 1-18.

Griffin, W.L.; Belousova, E.A.; Shee, S.R.; Pearson, N.J.; O´Reilly, S.Y. 2004. Archean crust evolution in the northern Yilgarn Craton: U-Pb and Hf-isotope evidence from detrital zircons. Precambrian Research 131: 231-282.

Iannizzotto, N.F.; Lopez de Luchi, M.G. 2012. Geotermobarometría en suites monzoníticas y graníticas de los batolitos devónicos de las Sierras de San Luis. Serie de Correlación Geológica 28: 39-52.

Iriarte, R.A.; Cordani, U.G.; Sato, K. 2021. Geochronology of the Cordillera Real granitoids, the inner magmatic arc of Bolivia. Andean Geology 48: 403-441. doi: http://dx.doi.org/10.5027/andgeoV48n3-3326

Kemp, A.I.S.; Hawkesworth, C.J.; Foster, G.L.; Paterson, G.A.; Woodhead, J.D.; Hergt, J.M.; Gray, C.M.; Whitehouse, M.J. 2007. Magmatic and crustal differentiation history of granitic rocks from Hf-O isotopes in zircon. Science 315: 980-983.

López de Luchi, M.G.; Siegesmund, S.; Wemmer, K.; Nolte, N. 2017. Petrogenesis of the postcollisional middle devonian monzonitic to granitic magmatism of the Sierra de San Luis, Argentina. Lithos 288-289: 191-213.

Ludwig, K.R. 2008. Isoplot/Ex 4.15. A Geochronological Toolkit for Microsoft Excel. Berkeley Geochronological Center, Berkely, Special publication 4: 76 p.

Macchioli Grande, M.; Alasino, P.; Dahlquist, J.; Morales Cámera, M.; Galindo, C.; Basei, M. 2020. Thermal maturation of a complete magmatic plumbing system at the Sierra de Velasco, Northwestern Argentina. Geological Magazine 158: 537-554.

Miller, J.S.; Matzel, J.E.P.; Miller, C.F.; Burgess, S.D.; Miller, R.B. 2007. Zircon growth and recycling during the assembly of large, composite arc plutons. Journal of Volcanology Geothermal Research 167: 282-299.

Morales Cámera, M.M.; Dahlquist, J.A.; Moreno, J.A.; Zandomeni, P.S.; García-Arias, M.; Basei, M.A.S. 2020. The Andaluca plutonic unit, Vinquis Intrusive Complex, Argentina: An assessment of mantle role in the genesis of Early Carboniferous weakly peraluminous A-type granites in the pre-Andean SW Gondwana margin. Lithos: 106873.

Moreno, J.A.; Dahlquist, J.A.; Morales Cámera, M.M.; Alasino, P.H.; Larrovere, M.A.; Basei, M.A.S.; Galindo, C.; Zandomeni, P.S.; Rocher, S. 2020. Geochronology and geochemistry of the Tabaquito batholith (Frontal Cordillera, Argentina): geodynamic implications and temporal correlations in the SW Gondwana margin. Journal of Geological Society of London 177: 455-474.

Morosini, A.F.; Ortiz Suárez, A.E.; Otamendi, J.E.; Pagano, D.S.; Ramos, G.A. 2017. La Escalerilla pluton, San Luis Argentina: the orogenic and post-orogenic magmatic evolution of the famatinian cycle at Sierras de San Luis. Journal of South American Earth Sciences 73: 100-118.

Muñoz, B.L.; Enriquez, E.; Morosini, A.F.; Demartis, M.; Ortiz Suárez, A.E.; Pinotti, L.; D'Eramo, F.J.; Christiansen, R.O.; Basei, M.A.S.; Grosso Cepparo, P.M.; Pagano, D.S.; Ramos, G.A. 2022. Age of the El Hornito pluton and thermobarometry of its thermal aureole: Insights into Achalian (Devonian) magmatism in the Sierras Pampeanas of Argentina. Journal of South American Earth Sciences 114. doi: https://doi.org/10.1016/j.jsames.2021.103705

Rapela, C.W.; Pankhurst, R.J.; Casquet, C.; Baldo, E.; Saavedra, J.; Galindo, C.; Fanning, C.M. 1998. The Pampean orogeny of the south proto-Andes: evidence for Cambrian continental collision in the Sierras de Cordoba. *In* The Proto-Andean Margin of Gondwana (Pankhurst, R.J.; Rapela, C.W.; editors). Special Publication Geological Society 142: 181-217. London.

Sato, A.M.; González, P.D.; Petronilho, L.A.; Llambías, E.J.; Varela, R.; Basei, M.A. 2001. Sm-Nd, Rb-Sr and K-Ar age constraints of the El Molle and Barroso plutons, western Sierra de San Luis, Argentina. *In* South America Symposium on Isotope Geology, No. 3, Extended Abstract Volume (CD). Sociedad Geológica de Chile: 241-244. Santiago.

Semenov, I.; Weinberg, R.F. 2017. A major mid-crustal decollement of the Paleozoic convergent margin of western Gondwana: the Guacha Corral shear zone, Argentina. Journal of Structural Geology 3: 75-99.

Siégel, C.; Bryan, S.E.; Allen, C.M.; Gusta, D.A. 2018. Use and abuse of zircon-based thermometers: A critical review and a recommended approach to identify antecrystic zircons. Earth-Sciences Review 176: 87-116.

Siegesmund, S.; Steenken, A.; López de Luchi, M.G.; Wemmer, K.; Hoffmann, A.; Mosch, S. 2004. The Las Chacras-Potrerillos batholith (Pampean Ranges, Argentina): structural evidence, emplacement and timing of the intrusion. Internationl Journal of Earth Sciences 93: 23-43.

Söderlund, U.; Patchett, J.P.; Vervoort, J.D.; Isachsen, C.E. 2004. The ^{176}Lu decay constant determined by Lu-Hf and U-Pb isotope systematics of Precambrian mafic intrusions. Earth Planetary Science Letters 219: 311-324.

Steiger, R.H.; Jager, E. 1977. Subcommission of geochronology: convention on the use of decay constants in geo- and cosmochronology. Earth Planetary Science Letters 36: 359-362.

Steenken, A.; López de Luchi, M.G.; Martínez Dopico, C.; Drobe, M.; Wemmer, K.; Siegesmund, S. 2011. The Neoproterozoic-Early Paleozoic metamorphic and magmatic evolution of the Eastern Sierras Pampeanas: An overview. *In* Multiaccretional Tectonics at the Rio de La Plata Margins (Siegesmund, S.; Basei, M.; Oyhantcabal, P.; editors). International Journal of Earth Sciences 100: 465-488. Berlin

Stuart-Smith, P.G.; Camacho, A.; Sims, J.P.; Skirrow, R.G.; Lyons, P.; Pieters, P.E.; Black, L.P. 1999. Uranium-lead dating of felsic magmatic cycles in the southern Sierras Pampeanas, Argentina: Implications for the tectonic development of the Proto-Andean Gondwana margin. *In* Laurentia Gondwana Connections before Pangea (Ramos, V.A.; Keppie, J.D.; editors). Geological Society of America, Special Paper 336: 87-114. McLean.

Manuscript received: November 28, 2022; revised/accepted: January 30, 2023; available online: January 31, 2023.
Editorial handling: Luis Lara.